Journal of Materials Chemistry C

Accepted Manuscript

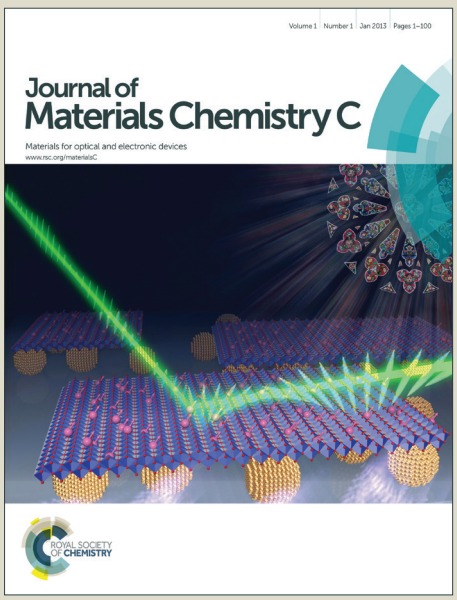

This is an *Accepted Manuscript*, which has been through the Royal Society of Chemistry peer review process and has been accepted for publication.

Accepted Manuscripts are published online shortly after acceptance, before technical editing, formatting and proof reading. Using this free service, authors can make their results available to the community, in citable form, before we publish the edited article. We will replace this *Accepted Manuscript* with the edited and formatted *Advance Article* as soon as it is available.

You can find more information about *Accepted Manuscripts* in the Information for Authors.

Please note that technical editing may introduce minor changes to the text and/or graphics, which may alter content. The journal's standard Terms & Conditions and the Ethical guidelines still apply. In no event shall the Royal Society of Chemistry be held responsible for any errors or omissions in this *Accepted Manuscript* or any consequences arising from the use of any information it contains.

ROYAL SOCIETY OF CHEMISTRY

www.rsc.org/materialsC

Photoluminescence properties of rare earth (Nd, Yb, Sm, Pr)-doped CeO_2 pellets prepared by solid-state reaction

Matteo Balestrieri, Silviu Colis*, Mathieu Gallart, Guy Schmerber, Marc Ziegler, Pierre Gilliot, and Aziz Dinia

Institut de Physique et Chimie des Matériaux de Strasbourg, Université de Strasbourg, CNRS UMR 7504, 23 rue du Loess, B.P. 43, F-67034 Strasbourg Cedex 2, France

Keywords: CeO_2, ceria, rare earths, downshifting, down-conversion

Abstract

Several structural and optical properties of ceria (band gap, refractive index and lattice parameter) make this material very promising for applications in optoelectronics and photovoltaics. In this paper, we show that CeO_2 can be efficiently functionalized by doping with trivalent rare earth ions to give rise to photon management properties. The trivalent ions can be successfully inserted by solid-state reaction of the elementary oxide powders. By combining the information obtained from the absorbance spectra with that of the PL excitation spectra, we demonstrate the presence of the trivalent ions in CeO_2 and provide insight in the electronic level structure and transfer mechanism. In particular, we prove that both the complex absorption spectra and the energy transfer mechanisms cannot be fully explained without considering the presence of isolated Ce^{3+} ions in CeO_2.

Introduction

Cerium(IV) oxide (also known as CeO_2 or ceria) is a widely used material due to its interesting chemical, mechanical and magnetic properties. It finds applications in catalysis, [1-3] in polishing, [4] in automobile exhaust catalysts [5] and as solid electrolyte in solid oxide fuel cells. [6, 7] Most of these applications of CeO_2 depend directly on properties induced by non-stoichiometry and the presence of the related point defects, such as oxygen vacancies and Ce^{3+} ions.

The most popular model describes CeO_2 as mixed-valence: the valence at the Ce site fluctuates between Ce^{3+}, $4f^1(v)$, with a vacancy (v) in the valence states of oxygen 2p and Ce^{4+}, $4f^0$. [8-14] The configuration interaction between the two valences best describes the electronic structure of the system. The 4f electron occupation value can be as high as 0.4-0.5. This mixed valence is characteristic of other rare earth oxides (Tb, Pr) and explains their particularly rich phase diagrams. [15] Experimental evidence of the mixed valence can be found in the analysis of the 3d photoemission spectra [16] and (with particularly high electron occupation values of the 4f band) in the paper of Aškrabić *et al.* [17] on nanocrystalline CeO_2. In fact, nanostructured CeO_2 tends to release more oxygen than bulk CeO_2 due to the increased surface-to-volume ratio.

A theoretical approach for calculating the band structure using the HSE (from Heyd, Scuseria, and Ernzerhof) hybrid functional theory has been proposed by Hay *et al.* [18] Their work is particularly interesting because it compares stoichiometric crystals of CeO_2 and Ce_2O_3. It also shows that for both oxides there are three bands close to the Fermi level and that all three are a hybrid of O 2p, Ce 4f and Ce 5d states. The 6s states are not considered because they are quite spread in energy and the density of states is low. However, they are expected to mix with the 5d states.

The lowest electronic transitions observed in CeO_2 are those between the O 2p occupied states and

the Ce 4f empty states. The calculated value (3.3 eV [18]) is smaller than the experimental value of 3.6 eV, [19-21] but considering that most density-functional theory (DFT) models strongly underestimate the band gap energy, [18] the agreement between the two values is acceptable.

The band gap of Ce_2O_3 (2.4 eV [22]) can be identified with the gap separating the partially filled Ce 4f and the Ce 5d6s electronic levels. The presence of 4f states between the O 2p and the Ce 5d6s band is characteristic of Ce and makes the band gap smaller than that associated with O 2p – Ce 5d6s transitions in other RE oxides (5.5–6.5 eV [23-25]).

Not all interesting properties of CeO_2 originate from its non-stoichiometry. For instance, the transparency to visible light and the refractive index value (slightly higher than 2 [26, 27]) are similar to those of large band gap semiconductors like ZnO, GaN, ITO (indium-tin oxide) and SnO_2, suggesting potential applications of CeO_2 in photovoltaics and optoelectronics. This material is particularly promising for application in silicon-based devices, thanks to the very good match of its lattice constant with that of Si. [28] The large absorption cross section in the UV region of the spectrum ascribes CeO_2 as a potential candidate sensitizer in the down-conversion process of UV photons.

CeO_2 is a promising host material for photon management also for other reasons, such as its good thermal and chemical stability, the small phonon energy compared to other oxides (465 cm^{-1} ≈ 58 meV) [29, 30], and the large ionic radius of Ce^{4+} (~90 pm), [31] which might favor the insertion of dopants.

Due to the empty 4f shell, Ce^{4+} ions do not have the rich energy level diagram that characterizes the rare earth (RE) ions. Therefore, the photon management properties can only be obtained by doping with other rare earth ions. If efficient energy transfer to the lanthanide dopant occurs, CeO_2 can be a good host for photon conversion. When a trivalent lanthanide substitutes a Ce^{4+} ion, the symmetry of the lattice site is lowered. [32, 33]

Compared to other RE doped oxide phosphors like glasses and ceramic materials, RE doping into CeO_2 in view of photon conversion has been relatively less studied. Recently, the UC properties have been investigated by Wu *et al.* [34] in three-dimensionally ordered macroporous CeO_2: Er^{3+}, Yb^{3+}, while the structural and luminescent properties of CeO_2:Eu^{3+} and CeO_2:Sm^{3+} thin films have been investigated by Fujihara and Oikawa [35] and by Wang *et al.* [36]. Additional work has been done by Kunimi and Fujihara, [37] Wang *et al.* [38] and Tiseanu *et al.* [32]

In this work, the structural and optical properties of RE-doped (RE = Pr, Nd, Yb, Sm) CeO_2 pellets prepared by solid state reaction of the elementary oxide powders are presented. The objective is not to perform an individual study of each rare earth with respect to the preparation conditions, but rather to compare different rare earths and try to obtain some information on the transfer mechanisms. Indeed, thanks to the thorough analysis of the absorbance and photoluminescence spectra, key information on the optical activation of the dopants and on the transfer mechanisms from the host have been obtained. We provide experimental evidence suggesting that the energy transfer occurs thanks to isolated Ce^{3+} ions in CeO_2 and not to the charge transfer mechanism between the O 2p band and the Ce 4f band as proposed by other authors. [32, 39]

Experimental

The preparation of CeO_2(:RE) pellets was carried out by solid state reaction of the oxides from the stoichiometric mixture of the elemental oxide powders. The indicated concentrations are the nominal concentrations. Indeed, the measurement of the concentration of elements that are so close in the periodic table and in low concentration is quite difficult by most of the common techniques, such as RBS and EDX.

Except for CeO_2 (Sigma Aldrich®, 99.95% pure) and Pr_2O_3 (Alfa Aesar®, 99.9% pure), all other oxides

have been prepared starting from RE salts. These salts have been thermally decomposed in air using tubular furnaces. Yb_2O_3 was prepared by decomposing Yb-oxalate ($Yb_2(C_2O_4)_3$) in air at 700 °C during 1h, as suggested by Hussein and Balboul. [40] The oxalate has been prepared by mixing a solution of Yb-acetate ($Yb(C_2H_3O_2)_3 \cdot xH_2O$, Sigma Aldrich®, 99.999% pure) with a solution of oxalic acid. The precipitate was then dried overnight at 50 °C before annealing. In the case of Nd_2O_3, Nd-nitrate hexahydrate ($Nd(NO_3)_3 \cdot 6\ H_2O$, Fluka®, 99.9 % pure) has been decomposed at several temperatures up to 1200 °C. Such high temperatures were reached using a Lenton® furnace. In the case of Sm_2O_3, Sm-nitrate hexahydrate ($Sm(NO_2)_3 \cdot 6\ H_2O$, Fluka®, >98 % pure) has been decomposed at 750 °C in air into a tubular furnace during 1h.

The exact weight ratios between CeO_2 and the rare earth sesquioxides have been calculated in order to attain the desired nominal concentration *x* (with respect to the Ce content). 4 g of powders are necessary to give after sintering round pellets of about 18 mm in diameter and 2 mm in height. The powders were carefully mixed in a mortar by adding few ml of ethanol and then let dry. The mix was then re-grinded in the mortar, pressed in a mold (26 mm of diameter) at 100 bars during 5 minutes and let dry overnight at 50 °C. The pellets were further placed into a Lenton® furnace where the temperature was increased up to 1400 °C at 1.6 °/min, followed by a dwell of 10 h at 1400 °C and a slow cooling down to room temperature.

The structural properties of the films were analyzed in the 20°–90° 2θ range by means of a Siemens® D5000 X-ray diffractometer equipped with a monochromated source delivering a Cu Kα1 incident beam (35 kV, 25 mA, λ = 0.154056 nm).

Photoluminescence (PL) measurements were performed in order to have insight on the insertion and activation of RE in CeO_2 as well as on the electronic level structure of RE^{3+} ions and on the energy transfer from CeO_2 to RE ions. The excitation was provided both by the 325 nm line of a He-Cd laser and a broad-spectrum Energetiq® EQ-99FC laser-driven light source (LDLS™) equipped with a monochromator. The signals were recorded by means of an N_2-cooled CCD camera.

Particular attention was paid to eliminate parasitic luminescence coming from the environment and from the excitation by using a set of filters. The spectra presented here have been corrected for the filter and lamp emission, as well as for the detector response.

Results and discussion

Cerium dioxide (CeO_2) has a cubic fluorite-type structure with a lattice constant *a* of 5.411 Å. Ce^{4+} ions are coordinated to 8 oxygen atoms in a cubic O_h symmetry. [41]

Figure 1 reports the XRD patterns of the CeO_2 powder, of the undoped pellet and a doped (Nd 3 %) pellet after sintering at 1400 °C. All peaks can be attributed to the cubic CeO_2 structure. No spurious phases containing Ce are observed in the detection limit of the XRD technique. For the pellets doped at 5 and 10 % with Sm, few small peaks related to Sm_2O_3 are detected. This indicates that part of the rare earths stay in the sesquioxide and do not migrate into CeO_2 during the solid state reaction.

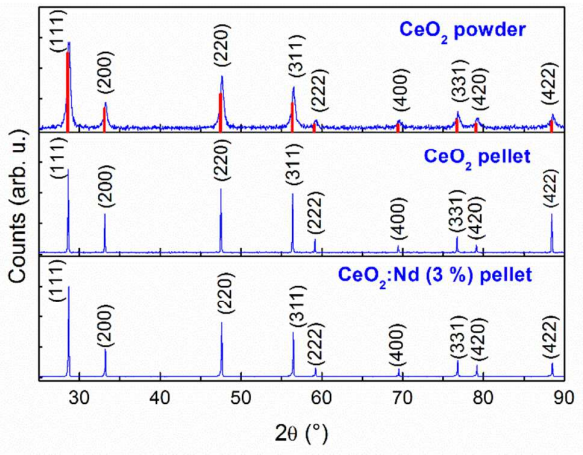

Figure 1 – XRD patterns of the CeO_2 powder and of the sintered pellets. Doping was found to induce no modification of the diffractogram and therefore only one pattern is reported (Nd 3%). The theoretical pattern (JCPDS 00-043-1002) is superimposed with the diffractogram of the powder for reference.

Information on the crystal quality of the pellets can be obtained by calculating the crystallites size and the lattice parameter. The values of the peak positions, corrected by the zero shift caused by the different thickness of the pellets, were obtained by least square method using all the peaks in the diffractogram. The lattice parameter calculated using Bragg's law and the values of the crystallites size calculated using Scherrer's formula on the (111) peak are reported in Table 1. The lattice parameter is close to the theoretical value of 5.41143 Å and the crystallites size increases 4 to 5 times with respect to the value in the powder. The error on the crystallites size is quite large, so that no conclusion can be drawn on the effect of the doping concentration. However, at such high temperatures and given the small mismatch of ionic radius between Ce and the other rare earths, the effect should be small.

Table 1 – Calculated values of the crystallites size and lattice parameter *a* of the CeO_2 pellets after sintering at 1400 °C. The crystallites size was calculated on the (111) peak, while the lattice parameter using all peaks. The values of the powder are reported for reference.

	Crystallites size (nm)	***a* (Å)**
Powder	18 ± 5	5.411 ± 0.002
Undoped	104 ± 16	5.414 ± 0.002
Yb (1 %)	91 ± 12	5.412 ± 0.002
Pr (1 %)	96 ± 14	5.412 ± 0.002
Nd (2 %)	81 ± 6	5.413 ± 0.002
Nd (3 %)	114 ± 19	5.414 ± 0.002
Sm (5 %)	73 ± 15	5.413 ± 0.002
Sm (10 %)	77 ± 17	5.408 ± 0.002

The XRD analysis confirms that the pellets are mainly composed of cubic CeO_2 crystallites, but gives no information about the rare earth insertion in the CeO_2 lattice. Evidence of insertion can be obtained from the investigation of the optical properties. The first optical observation on the pellets can be made by the naked eye. Contrarily to the snowy white CeO_2 powder, after sintering all pellets acquire a reddish color, ranging from a light orange hue to an intense copper-like color. This color is

the characteristic color of Ce_2O_3 and is due to the small band gap (2.4 eV [22]) of this oxide, although no trace of Ce_2O_3 has been observed in the XRD patterns. The measurement of the diffuse reflectance should allow discriminating if this color is due to the presence of Ce_2O_3 or to the absorption or emission from some impurities or intrinsic defects in CeO_2. Figure 2 reports the absorbance curves calculated from the diffuse reflectance of some of the pellets and of the CeO_2 powder.

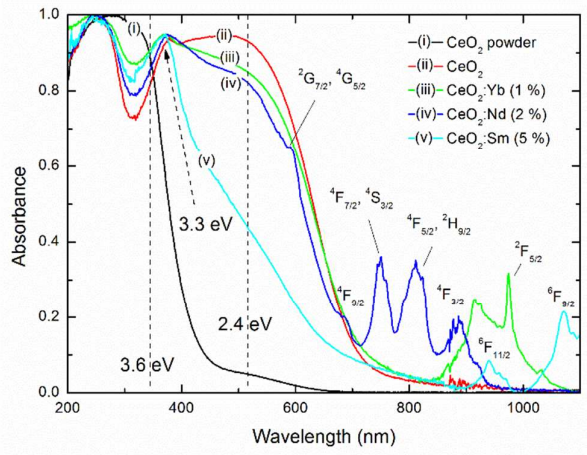

Figure 2 - Selected absorbance spectra calculated from the diffuse reflectance of the pellets and of the CeO_2 powder. The dopant-related absorption lines are labeled by the excited state to which the electron is promoted from the fundamental state of the trivalent RE^{3+} ion.

By looking at the spectrum of the powder reference, we see that the absorption edge is not as abrupt and it extends below the usually reported gap of 3.3-3.6 eV. [20] The high amount of surfaces in the powder and the associated high number of internal reflections might explain this behavior. In addition, a small absorption shoulder can be noticed around 2.4 eV.

In the case of the pellets, the absorption band extends well below the typical absorption edge of CeO_2. In particular, two additional wide absorbance features are observed (one at 3.3 eV and the other at 2.4 eV), which cover the whole spectrum below 600 nm and justify the reddish color of the pellets. These two features have been already observed by Tiseanu *et al.*, [32] but the authors do not provide any explanation for the band at 2.4 eV and attribute the band at 3.3 eV to the O^{2-} - Ce^{4+} charge transfer (CT) between the O 2p and the Ce 4f bands. However, the experimental range they use (>380 nm) prevents them from observing the third band observed in Fig. 2 for both the powder and the pellets, which is situated above 3.6 eV. The energy of this band is above that expected from O 2p / Ce 4f transitions and too low to arise from the excitation of O 2p electrons to the conduction band of CeO_2, which is mainly composed of unoccupied 5d and 6s states of Ce^{4+} and is expected above 5.5 eV. [25]

The origin of the high-energy absorption bands will be discussed with more details further in the paper.

The band at 3.3 eV is relatively narrow and is centered at about 380 nm (3.3 eV). Instead of the O^{2-} - Ce^{4+} charge transfer, we propose to attribute this band to f-d transitions on isolated Ce^{3+} ions in CeO_2. This energy is slightly lower than that expected for this kind of transitions, [35, 42] but this attribution is comforted by the fact that the energy position of the excited 5d state is easily affected by the local environment and thus depends on the preparation conditions. [32] In particular, the wavelength of the dipole allowed and fast 5d-4f emission in Ce^{3+} may vary from as short as 250 nm in fluoride compounds to 600 nm in sulfide compounds. [43] An additional consideration that supports this

hypothesis is that since f-d transitions in Ce^{3+} are dipole-allowed, even a small amount of ions can generate a strong absorption band.

It is worth noting that this band is not observed in the original powder. However, given the small crystallites size, the powder has probably been prepared at a lower temperature than 1400 °C. The reduced crystal order could make this band wider and the superposition with the other absorption bands could explain both why this band cannot be easily separated from the other bands and why the absorption edge is less abrupt than expected.

The good match with the band gap of Ce_2O_3 suggests that the absorption band at 2.4 eV is due to this oxide. The band is particularly strong in the undoped and low-doped pellets and extends at energies as low as 1.8 eV. Even if Ce_2O_3 is expected to have an indirect gap, [18] the absorption should not extend so low in energy. It is possible that Ce_2O_3 exists in amorphous phase, but since no literature has been found on amorphous Ce_2O_3, we have no comparison for the band gap value. The presence of Ce_2O_3 would indicate that a non-negligible amount of oxygen is lost during sintering even if the process occurs in air. This is not surprising, given the well known high mobility of oxygen in CeO_2 and the fact that CeO_2-based materials are already used for oxygen storage, thanks to the excellent oxygen vacancy formation and refilling capability. [44, 45] When an oxygen vacancy is formed, in order to balance the charge two neighboring Ce ions are reduced to 3+. The decrease of the absorption band at 2.4 eV with doping could be explained by the fact that the trivalent dopant ions contribute to balance the charge induced by the oxygen vacancies, thus requiring the formation of less Ce^{3+} ions.

Figure 2 also shows several absorption bands above 600 nm, related to 4f transitions of RE ions. The position of the bands proves that the dopants are in their 3+ state. No absorption from Pr^{3+} has been detected and the relative spectrum is therefore not reported. This might indicate that this rare earth exists in its 4+ state, favored by the presence of Ce^{4+}. Such a behavior has already been observed in Pr-doped ZnO. [46]

The PL spectra have been recorded in order to investigate the emission spectrum of the trivalent RE ions and of the CeO_2 matrix. Figure 3 shows the PL emission spectra of selected CeO_2 pellets under 325 nm He-Cd laser excitation. Unexpectedly, the emission spectrum of the undoped CeO_2 pellet is very rich. Several strong emission bands can be observed, composed of a large number of narrow peaks. Such an emission spectrum is typical of trivalent RE ions with a rich energy level diagram. Since none of these peaks can be attributed to Ce^{3+} ions, that have only one excited state about 0.3 eV above the fundamental state, or to CeO_2, indirect excitation of some rare earth impurities by energy transfer from the host must occur. Given the high purity of the powder (99.95 %), the overall impurity concentration must be below 0.05 %. Still, intense PL signals are recorded, suggesting that almost all ions are optically active and that the energy transfer is very efficient. The observed emission bands in the visible region of the spectrum can be attributed to Sm^{3+} impurities, [36] while the near infrared bands can be attributed to Nd^{3+}. [47] Most emission bands could be attributed to the specific 4f transitions, but a complete deconvolution of the spectra is a very hard task, due to the superposition of some Sm^{3+} emission lines with those of Nd^{3+} in the infrared region and to the very large number of peaks probably related to the existence of several active sites. Intentional doping with Sm and Nd at higher concentration strongly increases the emission (note the logarithmic scale). As expected, the increase of the PL is not proportional to the rare earth concentration over such a wide concentration range. Doping with Yb adds an emission band centered at 975 nm, which can be associated to $^2F_{5/2} \rightarrow {}^2F_{7/2}$ transitions in Yb^{3+}. [48, 49] Doping with Pr does not lead to new emission lines.

It also turns out that doping with Sm at 10 % leads to optical quenching of the emission. These data have been omitted from Figure 3 for clarity purposes.

It is interesting to notice that no emission has been recorded between 350 and 550 nm, where the excited Ce^{3+} ions should relax through 5d → 4f radiative transitions. Given the expected high concentration of Ce^{3+}, this effect might be due to concentration quenching. Alternatively, this might also indicate that most Ce^{3+} ions transfer their energy to the dopants. This would be the case if the presence of RE^{3+} in CeO_2 was often accompanied by that of Ce^{3+} in close proximity. The existence of rare earth ions dimers and triplets in charge compensated materials has been already observed [50] and might be particularly favored in CeO_2 thanks to the high mobility of the oxygen vacancies (which can virtually "move" the Ce^{3+} ions). Unfortunately, the difficulty to have (rare earth) impurity-free rare earth oxide did not allow having a pure CeO_2 pellet for comparison.

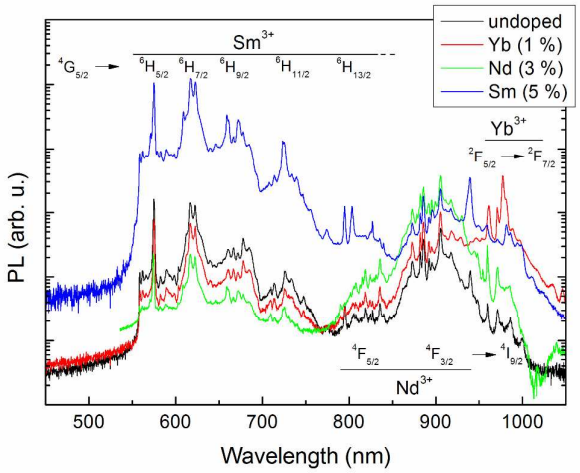

Figure 3 - PL emission spectra of the undoped and RE-doped CeO_2 pellets under 325 nm laser excitation (logarithmic scale).

The fact that the peaks are so narrow suggests that the active sites present very small lattice disorder and that the phonon broadening is weak. This is different from what is obtained in non-rare earth based hosts, such as ZnO [46-48] and SnO_2. [51, 52] The large number of peaks is probably due to the Stark splitting and to the existence of several active sites. In the case of Nd and Sm, which have a rich energy level diagram and could be directly excited by the laser, it cannot be excluded that some peaks originate from RE_2O_3 particles. In the case of Yb, however, direct excitation by 325 nm light cannot occur and some kind of transfer from the host is necessary to observe an emission.

The presence of intense emission from all 4f transitions is an indication that most ions are in a site with lower symmetry with respect to the cubic symmetry of Ce sites in ceria. In fact, since the intermediate coupling the selection rules on *L* and *S* quantum number are relaxed, a cubic environment would favor only few magnetic dipole-allowed (ΔJ = 0, ±1 ; 0 <≠> 0) transitions such as the $^4G_{5/2} \rightarrow {}^6H_{5/2}$ or the $^4G_{5/2} \rightarrow {}^6H_{7/2}$ transitions in the case of Sm. The existence of all the transitions indicates that something in the local environment breaks the inversion symmetry and introduces some J mixing. The unavoidable presence of oxygen vacancies in CeO_2 and their high mobility suggest that most sites might be characterized by oxygen-related defects.

More insight in the transfer mechanisms can be obtained by the analysis of the PLE spectra of the RE^{3+} emission, where the PL intensity is recorded as a function of the excitation wavelength. Figure 4 reports the PLE spectra of the strongest emission lines of Yb^{3+}, Sm^{3+} and Nd^{3+} (respectively at 977,

617 and 905 nm). In the spectrum of Nd- and Sm-doped CeO_2, several absorption bands are observed originating from direct excitation of the trivalent ions, but in all cases the strongest emission is recorded following indirect excitation of the host. Indirect excitation mainly occurs by exciting the absorption feature observed at 3.3 eV, which had been ascribed to isolated Ce^{3+} ions. The narrow shape of this excitation band suggests that the electronic states of the absorber are relatively localized.

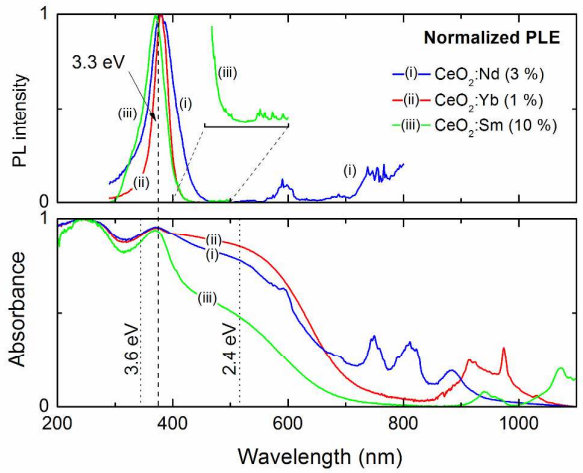

Figure 4 - PLE spectra of the main emission line of Yb^{3+}, Sm^{3+} and Nd^{3+}. The inset shows more clearly the direct excitation peaks of Sm^{3+} in CeO_2. The absorbance spectra are reported for reference.

In order to interpret these data correctly, Fig. 5 reports the experimental data of the CeO_2:Sm (5 %) pellet, for which the different bands are particularly well defined, and compares them to the theoretical calculations performed by Andersson *et al.* [53] and the different models proposed. We focus the attention on the two absorption bands denoted as (i) and (ii). Again, we see that the absorption band in the PLE spectrum corresponds to the absorption band denoted as (i). No energy transfer seems to occur from the band noted as (ii). It is worth noting that the shoulder observed in the PLE spectrum around 3.71 eV just above the main peak at 3.35 eV for the Sm-doped pellet is compatible with the splitting between the 4f levels of Ce^{3+} (about 300 meV [54]). This shoulder has already been observed by other authors. [35, 36, 39, 55]

Some authors, such as Tiseanu *et al.* [32] and Li *et al.*, [39] consider the transfer as occurring following O 2p / Ce 4f absorption in CeO_2. This mechanism, illustrated in Fig. 5b, involves the temporary reduction of Ce^{4+} to Ce^{3+} and could explain the two peaks observed in the PLE spectra by considering the two 4f excited states of Ce^{3+}. The relatively low energy (about 3.3 eV) of the transition compared to the previously reported gap of 3.6 eV is compatible with the trend observed by the above-mentioned authors for increased annealing temperatures in RE-doped CeO_2 nanoparticles. [39]

By plotting the absorption and the PL excitation spectra as a function of the energy and by setting the zero at the top of the valence band, we see that the model based on the O^{2-} - Ce^{4+} CT proposed for example by Tiseanu *et al.* [32] cannot fully explain the experimental data. In particular, with this model it is hard to explain the band marked as (ii). Since the authors do not consider the existence of intrinsic Ce^{3+}, the band can only be identified in the frame of the proposed mechanism by considering the lower states of the O 2p valence band (VB). However, such an explanation would be incompatible with the absence of energy transfer observed in the PLE spectrum following this excitation.

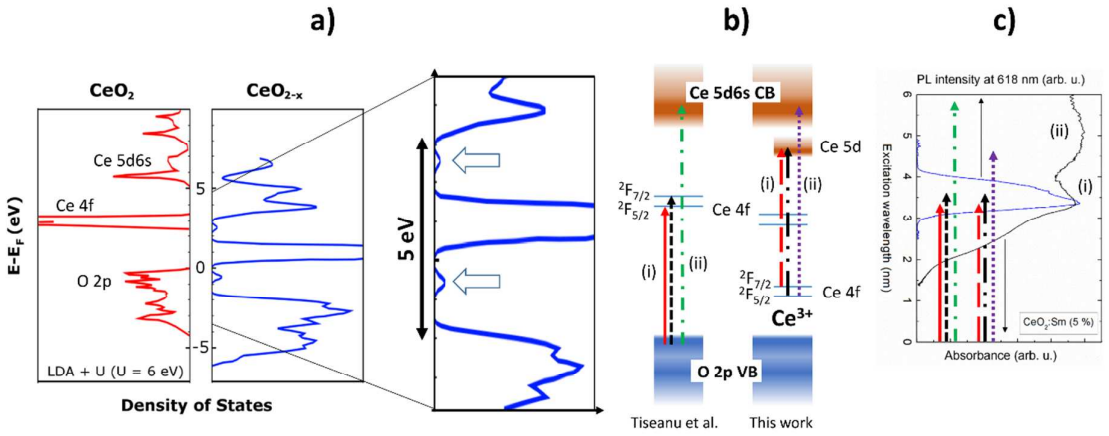

Figure 5 - a) Calculated DOS of CeO_2 and CeO_{2-x} using the LDA+U formalism. [53] A zoom in the energy region above the Fermi level shows that the theoretical results fit very well the model proposed in this paper (b) based on the PLE and absorbance spectra reported in (c) for the CeO_2:Sm (5 %) pellet, for which the different bands are particularly well defined. The vertical arrows indicate the possible absorption mechanisms.

The model proposed in this paper (see Fig. 5b), based on the PLE and absorbance spectra, attributes the absorption bands to electronic transitions from electrons in the partially filled 4f states created by isolated Ce^{3+} ions. If these states are situated about 1.2 – 1.5 eV above the O 2p valence band as indicated by other authors, [23, 56, 57] the proposed band structure fits very well with the calculated DOS of CeO_{2-x} using the LDA+U formalism by Andersson *et al.* [53] (see Fig. 5b). The existence of oxygen vacancies introduces some filled 4f states into the band gap between the O 2p states and the Ce 4f states, due to the presence of Ce^{3+} ions. At the same time, some Ce 5d states are introduced between the 4f states and the 5d6s states of Ce^{4+}. The amount and the exact position of these states probably depend on the x value and on the crystal order around the Ce^{3+} ion. This model has the advantage to explain the high energy absorption band (>4 eV) as a combination of the charge transfer of Ce^{3+} 4f localized electrons (roughly between 4.5 and 5.5 eV) to the Ce^{4+} 5d6s conduction band and of the O 2p / Ce 5d6s charge transfer (above 5.5 eV). With this in mind, the absence of energy transfer for high excitation energies can be easily understood, as the transfer would only occur from f-d transitions on localized Ce^{3+} ions and not when the electrons are promoted from isolated Ce^{3+} ions to the conduction band.

It is important to point out that following this mechanism, the two peaks of the PLE cannot be easily attributed to the 4f doublet. If this was the case, the main peak of the PLE spectrum (at 3.35 eV) should be attributed to f-d transitions from the 4f excited state of Ce^{3+} and not to its fundamental state. Since this excited state lays too high in energy to be thermally populated, this assumption should be made very carefully. Alternative explanations for the double peak might be a non-uniform energy distribution of the Ce^{3+} 5d electronic states or a contribution coming from the O^{2-} - Ce^{4+} CT mechanism.

In conclusion, the complex observed spectra could only be understood by taking into consideration the existence of intrinsic Ce^{3+} ions in CeO_2, which modifies the band structure. When discussing the CT mechanism to explain the energy transfer to Sm and Eu ions in CeO_2, Tiseanu *et al.* [32] and Li *et al.* [39] considered the existence of oxygen vacancies introduced by the dopant, but not the modified band structure induced by the consequent spontaneous creation Ce^{3+}.

In fact, the band between 300 and 400 nm is observed in other Ce^{3+}-doped materials. [55, 58, 59] This

fact supports the hypothesis of a cooperative downshifting process occurring on RE^{3+} ions situated close to Ce^{3+} ions.

This energy transfer mechanism based on f-d transitions on Ce^{3+} ions is illustrated in Figure 6. In the case of Sm and Nd, which have several levels in the same spectral region of the 5d band, it is probable that the transfer relies on the resonance with some level of the rare earth. Several resonances with different levels could explain the different shapes of the indirect transfer band of these two rare earths in Figure 4. On the other hand, Yb has no level in the same region, as the d shell is too high in energy and the single excited state is at only 1.3 eV above the fundamental state. Given the large energy mismatch between the bottom of the Ce^{3+} 5d shell (~ 3 eV) and the transition of Yb^{3+} (1.3 eV), phonon-assisted down-conversion might look improbable. However, relaxation through the $^2F_{7/2}$ excited state of Ce^{3+} could reduce this gap from a value of about 400 meV to about 100 meV, which is only twice the energy of the optical phonon in CeO_2. Such a process would occur within a narrow energy range, which could explain the relatively narrow excitation band for Yb in Figure 4. Some theoretical considerations on the Ce^{3+}-Yb^{3+} down-conversion process can be found in the work of Boccolini *et al*. [60] Although theoretically possible, time-dependent PL or quantum efficiency measurements are necessary to be sure that down conversion occurs and transfer through some deep defect level, such as those created by oxygen vacancies, [17] cannot be excluded at this stage.

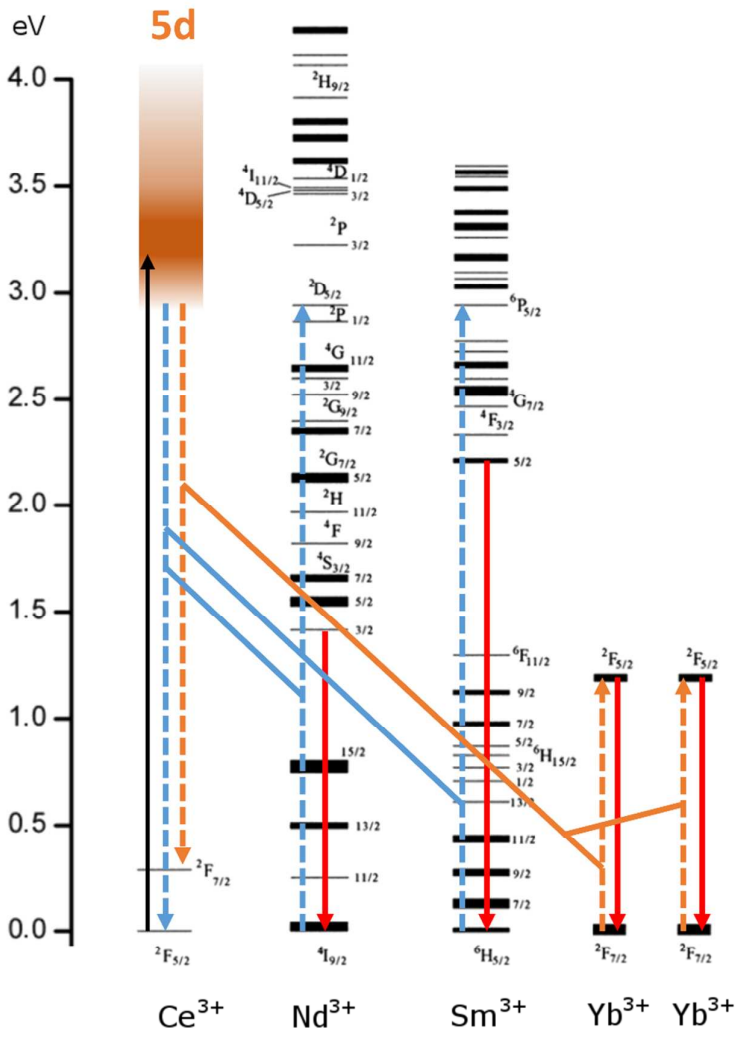

Figure 6 - Schematic of the possible energy transfer mechanisms in RE-doped CeO_2. The position of the energy levels of trivalent RE ions has been taken from ref. [54] and is relative to $LaCl_3$ as a host. The dashed arrows and the oblique lines represent the transfer mechanisms. The plain arrows correspond to some observed radiative transitions.

Conclusion

Except in the case of Pr, trivalent rare earth ions have been successfully inserted in CeO_2 by solid-state reaction of the elementary oxide powders. The structural analysis on the pellets showed that the rare earths do not modify the typical structure of CeO_2.

The different color observed for the pellets after sintering is due to the appearance of two absorption bands below the typical absorption band of CeO_2. By combining the information obtained from the absorbance with that of PL excitation spectra, and in agreement with the theoretical work carried out on the band structure of non-stoichiometric CeO_2, we interpret the different bands as follows. The higher band (below 300 nm) is composed of Ce^{3+} 4f / Ce^{4+} 5d charge transfer and of the O 2p / Ce 5d6s transitions. The band centered at 3.3 eV is attributed to f-d transitions on isolated Ce^{3+} ions. A contribution of O 2p / Ce 4f transitions is probably superimposed to this band in the absorbance spectrum.

The last band is centered at 2.4 eV and has been taken as indirect evidence of the presence of Ce_2O_3. Strong absorption bands composed of several narrow peaks have been also observed, arising from direct absorption on rare earth ions. The 4f transitions behind these bands have been identified and prove that these ions are in their trivalent form.

By combining the position of these narrow absorbance lines with the information obtained from the analysis of the PL and PLE spectra, most transitions have been identified. The emission from the dopants can be stimulated either by direct excitation or through the sensitizing absorption of the host. Surprisingly, the best sensitizer is not the host itself, but rather the f-d transitions on Ce^{3+} ions dispersed in it, due to the presence of oxygen vacancies. Given the indirect excitation process through Ce^{3+} ions, at least part of these trivalent RE ions have migrated into or in proximity of CeO_2.

In the case of Yb, the large energy gap between the f-d transition on Ce^{3+} and the 4f transition of Yb^{3+} suggests that the transfer might be more complicated. Relaxation through the 4f $^2F_{7/2}$ excited state of Ce^{3+} might favor a down-conversion process.

In this work we also showed that it is difficult to work with pure rare earth oxides and that the photoluminescence spectroscopy is a very powerful technique to study even very small rare earth concentrations (of less than 0.05 %).

Corresponding author

colis@ipcms.u-strasbg.fr, +33 3 88 10 71 29

Aknowledgements

The authors thank the Rhin Solar INTERREG project n° C25 and the French Ministry of Education and Research for financial support.

References

1. N. J. Lawrence, J. R. Brewer, L. Wang, T.-S. Wu, J. Wells-Kingsbury, M. M. Ihrig, G. Wang, Y.-L. Soo, W.-N. Mei and C. L. Cheung, *Nano Letters*, 2011, 11, 2666-2671.
2. B. Murugan and A. V. Ramaswamy, *J. Am. Chem. Soc.*, 2007, 129, 3062-3063.
3. A. D. Mayernick and M. J. Janik, *J. Phys. Chem. C*, 2008, 112, 14955-14964.
4. N. B. Kirk and J. V. Wood, *British Ceramic Trans.*, 1994, 93, 25–30.
5. B. R. Powell, R. L. Bloink and C. C. Eickel, *J. Am. Ceram. Soc.*, 1988, 71, C-104-C-106.
6. J. Van Herle, T. Horita, T. Kawada, N. Sakai, H. Yokokawa and M. Dokiya, *J. Am. Ceram. Soc.*, 1997, 80, 933-940.
7. W. Liu, B. Li, H. Liu and W. Pan, *Electrochim. Acta*, 2011, 56, 8329-8333.
8. T. K. Sham, R. A. Gordon and S. M. Heald, *Phys. Rev. B*, 2005, 72, 035113.
9. G. Krill, J. P. Kappler, A. Meyer, L. Abadli and M. F. Ravet, *J. Phys. F Met. Phys.*, 1981, 11, 1713-1725.
10. A. Bianconi, A. Marcelli, H. Dexpert, R. Karnatak, A. Kotani, T. Jo and J. Petiau, *Phys. Rev. B*, 1987, 35, 806-812.
11. H. Dexpert, R. C. Karnatak, J. M. Esteva, J. P. Connerade, M. Gasgnier, P. E. Caro and L. Albert, *Phys. Rev. B*, 1987, 36, 1750-1753.
12. T. Jo and A. Kotani, *Solid State Commun.*, 1985, 54, 451-456.
13. A. Kotani, T. Jo and J. C. Parlebas, *Adv. Phys.*, 1988, 37, 37-85.
14. M. Nakazawa, S. Tanaka, T. Uozumi and A. Kotani, *J. Electron Spectrosc.*, 1996, 79, 183-186.
15. G.-y. Adachi and N. Imanaka, *Chem. Rev.*, 1998, 98, 1479-1514.
16. T. Nakano, A. Kotani and J. C. Parlebas, *J. Phys. Soc. Jpn.*, 1987, 56, 2201-2210.

17. S. Aškrabić, Z. D. Dohčević-Mitrović, V. D. Araújo, G. Ionita, J. M. M. de Lima and A. Cantarero, *J. Phys. D Appl. Phys.*, 2013, 46, 495306 - 495306-9.
18. P. J. Hay, R. L. Martin, J. Uddin and G. E. Scuseria, *J. Chem. Phys.*, 2006, 125, 034712-1 - 8.
19. S. Colis, A. Bouaine, G. Schmerber, C. Ulhaq-Bouillet, A. Dinia, S. Choua and P. Turek, *Phys. Chem. Chem. Phys.*, 2012, 14, 7256-63.
20. S. Guo, H. Arwin, S. N. Jacobsen, K. Järrendahl and U. Helmersson, *J. Appl. Phys.*, 1995, 77, 5369-5376.
21. S. Colis, A. Bouaine, R. Moubah, G. Schmerber, C. Ulhaq-Bouillet, A. Dinia, L. Dahéron, J. Petersen and C. Becker, *J. Appl. Phys.*, 2010, 108, 053910 - 053910-6.
22. A. V. Prokofiev, A. I. Shelykh and B. T. Melekh, *J. Alloy Compd.*, 1996, 242, 41-44.
23. A. Pfau and K. D. Schierbaum, *Surf. Sci.*, 1994, 321, 71-80.
24. F. Marabelli and P. Wachter, *Phys. Rev. B*, 1987, 36, 1238-1243.
25. N. V. Skorodumova, R. Ahuja, S. I. Simak, I. A. Abrikosov, B. Johansson and B. I. Lundqvist, *Phys. Rev. B*, 2001, 64, 115108 - 115108-9.
26. R. M. Bueno, J. M. Martinez-Duart, M. Hernandez-Velez and L. Vazquez, *J. Mater. Sci.*, 1997, 32, 1861-1865.
27. K. Narasimha Rao, L. Shivlingappa and S. Mohan, *Mater. Sci. Eng. B-Solid*, 2003, 98, 38-44.
28. T. Inoue, Y. Yamamoto, S. Koyama, S. Suzuki and Y. Ueda, *Appl. Phys. Lett.*, 1990, 56, 1332-1333.
29. S. Wang, W. Wang, J. Zuo and Y. Qian, *Mater. Chem. Phys.*, 2001, 68, 246-248.
30. I. Kosacki, T. Suzuki, H. U. Anderson and P. Colomban, *Solid State Ionics*, 2002, 149, 99-105.
31. R. Shannon, *Acta Crystallogr. A*, 1976, 32, 751-767.
32. C. Tiseanu, B. Cojocaru, D. Avram, V. I. Parvulescu, A. V. Vela-Gonzalez and M. Sanchez-Dominguez, *J. Phys. D Appl. Phys.*, 2013, 46, 275302 - 275302-8.
33. C. Tiseanu, V. I. Parvulescu, M. Boutonnet, B. Cojocaru, P. A. Primus, C. M. Teodorescu, C. Solans and M. S. Dominguez, *Phys. Chem. Chem. Phys.*, 2011, 13, 17135-17145.
34. H. Wu, Z. Yang, J. Liao, S. Lai, J. Qiu, Z. Song, Y. Yang, D. Zhou and Z. Yin, *J. Alloy Compd.*, 2014, 586, 485-487.
35. S. Fujihara and M. Oikawa, *J. Appl. Phys.*, 2004, 95, 8002-8006.
36. L. Li, S. W. Wang, G. Y. Mu, X. Yin, Y. Tang, W. B. Duan and L. X. Yi, *Phys. Status Solidi B*, 2013, 251, 737–740.
37. S. Kunimi and S. Fujihara, *ECS J. Solid State Sci. Technol.*, 2012, 1, R32-R36.
38. X. Wang, D. Zhang, Y. Li, D. Tang, Y. Xiao, Y. Liu and Q. Huo, *RSC Adv.*, 2013, 3, 3623-3630.
39. L. Li, H. K. Yang, B. K. Moon, Z. Fu, C. Guo, J. H. Jeong, S. S. Yi, K. Jang and H. S. Lee, *J. Phys. Chem. C*, 2009, 113, 610-617.
40. G. A. M. Hussein and B. A. A. Balboul, *Powder Technol.*, 1999, 103, 156-164.
41. K. Nakamoto, *Infrared and Raman Spectra of Inorganic and Coordination Compounds*, John Wiley & Sons, New York, 5th edn., 1997.
42. X. Zhao, L. Fan, T. Yu, Z. Li and Z. Zou, *Opt. Express*, 2013, 21, 31660-31667.
43. P. Dorenbos and E. van der Kolk, *Proc. SPIE* 6473, Gallium Nitride Materials and Devices II, 647313 - 647313-10, San José, California, 2007.
44. H.-F. Wang, H.-Y. Li, X.-Q. Gong, Y.-L. Guo, G.-Z. Lu and P. Hu, *Phys. Chem. Chem. Phys.*, 2012, 14, 16521-16535.
45. A. Trovarelli, *Comment. Inorg. Chem.*, 1999, 20, 263-284.
46. M. Balestrieri, M. Gallart, M. Ziegler, P. Bazylewski, G. Ferblantier, G. Schmerber, G. S. Chang, P. Gilliot, D. Muller, A. Slaoui, S. Colis and A. Dinia, *J. Phys. Chem. C*, 2014, 118, 13775-13780.
47. M. Balestrieri, S. Colis, M. Gallart, G. Ferblantier, D. Muller, P. Gilliot, P. Bazylewski, G. S. Chang, A. Slaoui and A. Dinia, *J. Mater. Chem. C*, 2014, 2, 9182-9188.
48. M. Balestrieri, G. Ferblantier, S. Colis, G. Schmerber, C. Ulhaq-Bouillet, D. Muller, A. Slaoui and A. Dinia, *Sol. Energy Mater. Sol. Cells*, 2013, 117, 363-371.
49. I. Soumahoro, G. Schmerber, A. Douayar, S. Colis, M. Abd-Lefdil, N. Hassanain, A. Berrada, D. Muller, A. Slaoui, H. Rinnert and A. Dinia, *J. Appl. Phys.*, 2011, 109, 033708 - 033708-5.

50. M. B. Seelbinder and J. C. Wright, *J. Chem. Phys.*, 1981, 75, 5070-5079.
51. H. Rinnert, P. Miska, M. Vergnat, G. Schmerber, S. Colis, A. Dinia, D. Muller, G. Ferblantier and A. Slaoui, *Appl. Phys. Lett.*, 2012, 100, 101908 - 101908-3.
52. K. Bouras, J. L. Rehspringer, G. Schmerber, H. Rinnert, S. Colis, G. Ferblantier, M. Balestrieri, D. Ihiawakrim, A. Dinia and A. Slaoui, *J. Mater. Chem. C*, 2014, 2, 8235-8243.
53. D. A. Andersson, S. I. Simak, B. Johansson, I. A. Abrikosov and N. V. Skorodumova, *Phys. Rev. B*, 2007, 75, 035109 - 035109-6.
54. G. H. Dieke, *Spectra and Energy Levels of Rare Earth Ions in Crystals*, Interscience Publishers, New York, 1968.
55. J. Weimmerskirch-Aubatin, M. Stoffel, X. Devaux, A. Bouché, M. Vergnat and H. Rinnert, *Phys. Status Solidi C*, 2014, 11, 1630-1633.
56. D. R. Mullins, P. V. Radulovic and S. H. Overbury, *Surf. Sci.*, 1999, 429, 186-198.
57. M. A. Henderson, C. L. Perkins, M. H. Engelhard, S. Thevuthasan and C. H. F. Peden, *Surf. Sci.*, 2003, 526, 1-18.
58. J.-i. Nara and S. Adachi, *ECS J. Solid State Sci. Technol.*, 2013, 2, R135-R141.
59. A. Guille, A. Pereira, G. Breton, A. Bensalah-Ledoux and B. Moine, *J. Appl. Phys.*, 2012, 111, -.
60. A. Boccolini, J. Marques-Hueso, D. Chen, Y. Wang and B. S. Richards, *Sol. Energy Mater. Sol. Cells*, 2014, 122, 8-14.

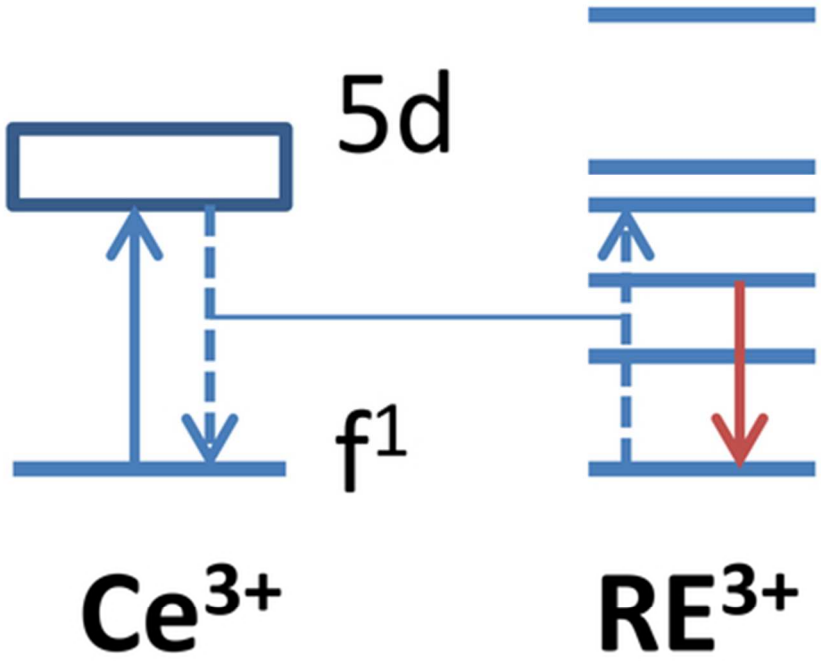

The luminescence of rare earths in CeO_2 is sensitized by intrinsic Ce^{3+} ions
39x32mm (300 x 300 DPI)